

Original Article

Cite this article: Laverick JH, Green TK, Burdett HL, Newton J, Rogers AD (2019). Depth alone is an inappropriate proxy for physiological change in the mesophotic coral *Agaricia lamarcki*. *Journal of the Marine Biological Association of the United Kingdom* **99**, 1535–1546. <https://doi.org/10.1017/S0025315419000547>

Received: 8 January 2019

Revised: 19 May 2019

Accepted: 20 May 2019

First published online: 24 June 2019

Key words:

Depth; heterotrophy; isotopes; mesophotic; photosynthesis; physiology

Author for correspondence:

Jack H. Laverick, E-mail: jacklaverick@gmail.com

Depth alone is an inappropriate proxy for physiological change in the mesophotic coral *Agaricia lamarcki*

Jack H. Laverick^{1,2}, Tamara K. Green³, Heidi L. Burdett^{4,5}, Jason Newton⁶
and Alex D. Rogers¹

¹Department of Zoology, University of Oxford, Oxford, UK; ²Operation Wallacea, Spilsbury, UK; ³School of Earth and Environmental Science, University of St Andrews, St Andrews, UK; ⁴Lyell Centre for Earth and Marine Science and Technology, Edinburgh, UK; ⁵School of Energy, Geoscience, Infrastructure and Society, Heriot-Watt University, Edinburgh, UK and ⁶NERC Life Sciences Mass Spectrometry Facility, SUERC East Kilbride, East Kilbride, UK

Abstract

The physiology of mesophotic Scleractinia varies with depth in response to environmental change. Previous research has documented trends in heterotrophy and photosynthesis with depth, but has not addressed between-site variation for a single species. Environmental differences between sites at a local scale and heterogeneous microhabitats, because of irradiance and food availability, are likely important factors when explaining the occurrence and physiology of Scleractinia. Here, 108 colonies of *Agaricia lamarcki* were sampled from two locations off the coast of Utila, Honduras, distributed evenly down the observed 50 m depth range of the species. We found that depth alone was not sufficient to fully explain physiological variation. Pulse Amplitude-Modulation fluorometry and stable isotope analyses revealed that trends in photochemical and heterotrophic activity with depth varied markedly between sites. Our isotope analyses do not support an obligate link between photosynthetic activity and heterotrophic subsidy with increasing depth. We found that *A. lamarcki* colonies at the bottom of the species depth range can be physiologically similar to those nearer the surface. As a potential explanation, we hypothesize sites with high topographical complexity, and therefore varied microhabitats, may provide more physiological niches distributed across a larger depth range. Varied microhabitats with depth may reduce the dominance of depth as a physiological determinant. Thus, *A. lamarcki* may ‘avoid’ changes in environment with depth, by instead existing in a subset of favourable niches. Our observations correlate with site-specific depth ranges, advocating for linking physiology and abiotic profiles when defining the distribution of mesophotic taxa.

Introduction

Mesophotic coral ecosystems (MCEs) are zooxanthellate coral reefs widely considered to occur from between 30–40 m to at least 150 m depth (Puglise *et al.*, 2009; Kahng *et al.*, 2014; Baker *et al.*, 2016b). Deeper reefs are typically darker, colder and further offshore (Lesser *et al.*, 2009). Recently, MCEs in the Caribbean have been recognized as their own distinct biological assemblage, characterized by the absence of shallow-specialist taxa and the presence of depth-generalists (Semmler *et al.*, 2016; Laverick *et al.*, 2017). The upper and lower boundaries of MCEs may therefore be considered variable, with distributions likely underpinned by physiological responses to the environment.

Photosynthetic scleractinian corals derive a significant portion of their energy from sunlight (Hatcher, 1988). However, as depth increases, photosynthetically active radiation (PAR) declines (Sathyendranath & Platt, 1988). The depth-generalist profile typical of mesophotic Scleractinia in the Caribbean (Semmler *et al.*, 2016; Laverick *et al.*, 2017) therefore poses a significant physiological challenge. Photosynthetic corals may increase their photosynthetic efficiency to accommodate changing light profiles (Anthony & Hoegh-Guldberg, 2003; Hennige *et al.*, 2008). This can be achieved through symbiont switching (Bongaerts *et al.*, 2015), increased symbiont densities (Bongaerts *et al.*, 2011) or pigment concentrations (Cohen & Dubinsky, 2015; Borell *et al.*, 2016), changing growth form (Graus & MacIntyre, 1982), or even by modifying the reflective properties of the coral skeleton (Enríquez *et al.*, 2017) with differences noted between shallow and mesophotic taxa (Kahng *et al.*, 2012). Additionally, scleractinian corals sit on a spectrum of mixotrophy, with variable rates of heterotrophic feeding (Palardy *et al.*, 2005). Heterotrophic subsidy may be used as a strategy to survive coral bleaching events, when the energy contribution from photosynthesis declines (Grottoli *et al.*, 2014). Heterotrophic subsidy, therefore, has also been recognized as a possible mechanism permitting the depth-generalist distribution of mesophotic hard corals (Alamaru *et al.*, 2009; Lesser *et al.*, 2010; Crandall *et al.*, 2016). A third conceivable physiological adaptation to low light levels is a reduced metabolic rate, and so energy requirement (Davies, 1980). Though mass specific respiration rates at rest (basal metabolic rates) appear remarkably



consistent across biology (Suarez *et al.*, 2004; Makarieva *et al.*, 2008), energy could be saved by reduced investment in reproduction (Feldman *et al.*, 2017; Shlesinger *et al.*, 2018) or growth.

Pulse Amplitude Modulated (PAM) fluorometry is an established method for studying photochemistry (Schreiber, 2004) and can be used to calculate a variety of metrics, such as photosynthetic efficiency and capacity, light-related stress, and other features (Jassby & Platt, 1976; Juneau *et al.*, 2005). Further, the ratios of heavy to light nitrogen isotopes in coral tissue can provide a measure of heterotrophic feeding (Peterson & Fry, 1987), providing environmental differences are accounted for (Heikoop *et al.*, 2000; Baker *et al.*, 2010). Discrimination between carbon isotopes is partly dependent on photosynthetic activity in the absence of feeding (Alamaru *et al.*, 2009); the translocation of carbon from the zooxanthellae symbionts to the coral host may be affected by depth and produce an isotopic signature (Muscatine *et al.*, 1989). However, lipid content may also affect bulk $\delta^{13}\text{C}$ measurements (Alamaru *et al.*, 2009).

Stable isotope analyses and PAM fluorometry of a number of mesophotic Scleractinia, including *Agaricia lamarcki* (Crandall *et al.*, 2016) and *Montastraea cavernosa* (Lesser *et al.*, 2010, 2014; Crandall *et al.*, 2016) in the Caribbean, and *Favia fava* (Alamaru *et al.*, 2009) and *Stylophora pistillata* (Alamaru *et al.*, 2009; Einbinder *et al.*, 2009; Brokovich *et al.*, 2010; Nir *et al.*, 2011; Cohen & Dubinsky, 2015; Einbinder *et al.*, 2016) in the Red Sea, have revealed between-species variation in the changing rate of heterotrophy and photosynthetic efficiency with depth. However, there has been little effort to investigate intra-species variation between sites with different abiotic conditions, such as light levels and slope.

The relationship between these factors and the cellular physiology of corals across depth gradients has also yet to be examined in detail. The intracellular ratio between the secondary metabolites dimethylsulphoxide and dimethylsulphoniopropionate (DMSO:DMSP) has been previously used as an early indicator for cellular oxidative 'stress' in the cordgrass *Spartina alterniflora* (Husband & Kiene, 2007; McFarlin & Alber, 2013) because of their role in cellular antioxidant cascades (Sunda *et al.*, 2002). Since corals (and associated symbionts) harbour significant quantities of DMSP (Raina *et al.*, 2013; Burdett *et al.*, 2014), it may be hypothesized that the DMSO:DMSP ratio is also a useful oxidative stress indicator for these organisms. Elevated DMSP concentrations have been observed coinciding with a stressful light environment for *S. pistillata* in the Red Sea (Borell *et al.*, 2016).

Here, we consider the physiology of the mesophotic depth-generalist scleractinian *A. lamarcki*, one of the dominant mesophotic taxa at our Caribbean study sites. *A. lamarcki* is a brooding species, which has shown limited symbiont switching around the mesophotic-shallow reef boundary (Bongaerts *et al.*, 2015). We sampled two sites down a continuous depth gradient to assess the consistency of physiological patterns with depth. We use techniques which have already been used to assess physiological change across the shallow-mesophotic depth gradient (Alamaru *et al.*, 2009; Einbinder *et al.*, 2009; Lesser *et al.*, 2010; Crandall *et al.*, 2016); PAM fluorometry, oxygen flux, stable isotope analyses, and also investigate trends in intracellular DMSP:DMSO ratios.

Materials and methods

Research site

Utila is one of the Honduran Bay Islands on the southern end of the meso-American barrier reef. A quantitative benthic description exists to a maximum depth of 85 m (Laverick *et al.*, 2017). Of the five sites described, two are considered here: 'The Maze' on the north shore (TMA, N 16.112, W-86.949, WGS84 format) and 'Little Bight' on the south shore (LB, 16.079, W-86.929).

Generally, south shore reefs are slopes ending in sand at ~45 m depth. In contrast, north shore reefs are typically walls extending deeper than 100 m. Though we do not have light data, the sites are known to have differing maximum depth ranges for *A. lamarcki* and the transition depths from shallow to mesophotic communities are known to be deeper at TMA than LB (Laverick *et al.*, 2017).

Collection

Coral fragments were collected (permit number: ICF-261-16) by scuba divers using mixed gas closed circuit rebreathers during July 2015. During collection dives, *A. lamarcki* colonies were identified as plating and encrusting agariciid colonies with white, star-shaped polyps (Humann & Deloach, 2013). Species identity was verified by the alternation of long and short septo-coxae following examination under a microscope in the field (Veron *et al.*, 2016).

Sampled depths were from 10 to 45 m at the site LB and 16 to 60 m at TMA. These depths reflect the shallowest and deepest observed colonies of *A. lamarcki* at each site. We are confident the whole depth range of *A. lamarcki* was sampled for the following reasons. The lower limit of LB coincides with a sandy plain, and concurrent ecological studies at TMA, which reported no Scleractinia deeper than 85 m with maximum dive depths of 100 m (Laverick *et al.*, 2017), did not report deeper incidences of *A. lamarcki* than sampled here. Additionally, roaming divers reported no *A. lamarcki* deeper than 60 m. Sampled coral colonies were >40 cm in diameter, to minimize damage to newly recruited colonies, and 5+ m from their nearest sampled neighbour to minimize the sampling of clones. All colonies were sampled as they were found, so long as they satisfied these selection criteria, with up to 12 colonies per 10 m vertical depth band. Half the samples were collected by swimming with the reef on the divers' left side from the dive site mooring buoy, half with the reef on the right side.

To sample a suitable colony, a thumb sized fragment was excised using a chisel from the plate margin. This was placed in a labelled zip-lock bag and stowed in a PVC tube that was opaque to light. Fragments were kept in the dark prior to analysis to mitigate light-associated stress during the divers' ascent. Once stowed, the fractured margin of the colony was lined with pre-mixed Milliput modelling putty to prevent infection or fouling (Downs, 2011). The samples were returned to a temperature-controlled field lab and placed within an opaque plastic aquarium filled with water from the fore-reef. The aquaria were heated to 28°C (= ambient *in situ* temperature), aerated, and covered in four layers of plastic tarp to allow dark acclimation of fragments. Samples were acclimated in the dark for 12 h prior to analysis for photosynthetic characteristics and dissolved oxygen consumption.

Water (LB N = 4, TMA N = 18) and sediment samples (LB N = 14, TMA N = 24) were collected from both sites at 5, 15, 25, 40, and also at 55 and 70 m at TMA. These samples provide an environmental isotope signature for context when interpreting the trends in coral values (Heikoop *et al.*, 2000; Baker *et al.*, 2010). Sediment was collected in sediment traps deployed on the reef for 4 weeks before the contents were drained and desiccated. Water was collected by scuba divers and poisoned in the lab with 10 μl of mercuric chloride solution per 12 ml of water, and stored without headspace in exetainer vials (Labco Ltd).

Laboratory methods

Oxygen incubations

Coral fragments were removed from their aquarium, in the dark, and isolated in 450 ml plastic chambers. Chambers were filled with fresh, unfiltered, seawater from the fore-reef in the same container, at the same time of day. The chambers were left for an

hour, deemed a suitable time for generating a detectable signal after pilot tests. The lab was kept in darkness during the incubations. Water samples were taken at the beginning and end of the incubation. The change in dissolved oxygen (DO₂) content was quantified using the same Fibox oxygen optode sensor spot system calibrated with a two-point calibration according to the manufacturer's instructions (PreSens Precision Sensing GmbH). The probe was held steady until the reading plateaued before recording. The change in dissolved oxygen during the incubation (ΔDO_2) was standardized to 10 g of coral tissue, measured when later removed from the fragment (details below), and to the hour.

PAM fluorometry

Immediately after the oxygen incubation, Rapid Light Curves (RLCs) were conducted on the submerged, polyp-bearing side of the coral fragment using PAR levels of 2, 3, 5, 8, 12, 19, 37, 64, 110 $\mu\text{mol m}^{-2} \text{s}^{-1}$ set on a Diving-PAM (Heinz Walz GmbH). The fibre optic was positioned 5 mm away from the coral surface using the Surface Holder attachment during all RLCs. PAR levels for the RLCs were chosen based on a balance between avoiding rapid light saturation of mesophotic fragments, whilst still achieving a detectable response from shallow fragments.

For RLCs a steady state is not reached during each light step (Ralph & Gademann, 2005), unlike traditional light curves. Therefore, results from RLCs yield information on the actual, rather than optimal, photosynthetic state as suggested by traditional light curves (Ralph & Gademann, 2005). Additionally, comparing RLCs from different species or under different environmental conditions should be conducted with care, as the irradiance absorption of a photosynthetic organism may change, affecting electron transport rates (Saroussi & Beer, 2007; Einbinder *et al.*, 2016). Comparisons between sites and/or depths may therefore be affected by changes in the coral's irradiance absorption, such as changes in coral optics (Chalker *et al.*, 1983; Anthony & Hoegh-Guldberg, 2003; Wangpraseurt *et al.*, 2019), and have been taken into account when interpreting the PAM fluorometry results. Our results represent an integrated photosynthetic and bio-optical response, providing relative comparisons of the same species between sites. Variations are likely to have arisen in response to a varied environmental regime, thereby enabling comparison between sites, albeit without the capacity to identify if any observed changes are as a result of photosynthetic or bio-optical characteristics.

Stable isotope analyses

All stable isotope samples were prepared as described below before shipping to the UK for analysis at the NERC Life Sciences Mass Spectrometry Facility in East Kilbride. In the field, following RLCs, coral fragments were patted dry and their mass recorded. Surface coral tissue was removed using a Waterpik filled with seawater (Johannes & Wiebe, 1970). The mass of the air-dried skeleton was later recorded to allow the mass of coral tissue to be determined (= original mass – mass of bare skeleton). Air-dried skeleton was ground into a powder using a pestle and mortar and sealed in micro-centrifuge tubes. Coral slurry was left to settle and then pipetted into micro-centrifuge tubes. The tubes were centrifuged at 14,000 rpm for 60 s and the supernatant removed. This was repeated three times, topping with more slurry between spins to maximize material recovery. The resulting material was left standing for 10 h, in an aluminium tray under a sheet of glass in direct sunlight, to allow desiccation before storing at -20°C . Upon return to the UK these samples, and sediments, were further dried at 50°C overnight. We were unable to separate symbiont and host tissue in the field, we therefore interpret our results at the level of the holobiont, as has been done in similar studies (Crandall

et al., 2016). When host and symbiont have been analysed independently, the results tend to show a shift in mean values between the two fractions, but similar relationships with increasing depth (Alamaru *et al.*, 2009; Einbinder *et al.*, 2009; Lesser *et al.*, 2010).

Sediments and tissue samples ($\delta^{15}\text{N}$, $\delta^{13}\text{C}$)

Samples were weighed (0.7 mg for organic tissues, 5 mg for sediment) into tin capsules and loaded into an Elementar (Hanau, Germany) Pyrocube elemental analyser (EA) run in NC mode. Samples were combusted and gases purified such that N₂ (for $\delta^{15}\text{N}$) and CO₂ (for $\delta^{13}\text{C}$) were admitted consecutively into a Thermo (Bremen, Germany) Delta XP isotope ratio mass spectrometer (IRMS). The protocol loosely follows simultaneous nitrogen, carbon and sulphur analysis (Fourel *et al.*, 2014) with the following deviations: we did not run for sulphur and so did not use a SO₂ trap; oxidation and reduction reactors were cooler at 950 and 600°C respectively; the oxidation reactor was centrally filled with CuO as a catalyst, succeeded by a plug of silver wool filtering Cl species. Three standards were used to correct for linearity and drift of a range of $\delta^{15}\text{N}$ and $\delta^{13}\text{C}$ (Werner & Brand, 2001; Newton, 2010): a gelatine solution (GEL), a ¹³C-enriched alanine/gelatine solution (ALAGEL), and a ¹⁵N-enriched glycine/gelatine solution (GLYGEL). All standard solutions were dispensed into tin capsules and oven dried at 70°C prior to analysis. C and N abundance, and an independent evaluation of isotope ratio, was provided by four USGS40 standards (Qi *et al.*, 2003). Measurement error of all four reference materials can be found in the supplementary information (Supplementary 1).

Dissolved inorganic carbon (DIC, $\delta^{13}\text{C}$)

Two drops of 103% phosphoric acid were added to exetainers (Labco Ltd), which were then flushed with helium. 1 ml of each water sample was added to the exetainer via a syringe through the septum. The phosphoric acid liberated gaseous CO₂ from the sample into the headspace of the exetainer. Standards were treated differently as these were solid sodium bicarbonate and calcium carbonate powders (Waldron *et al.*, 2014). Standards were loaded into dry exetainers with 1 ml of dilute phosphoric acid, ensuring the H₃PO₄ concentration was the same as for the samples. For both standards and samples, the headspace CO₂ was dried in a Gas Bench (Thermo, Bremen, Germany) and the $\delta^{13}\text{C}$ measured on a Thermo (Bremen, Germany) Delta V IRMS (Torres *et al.*, 2005; Yang & Jiang, 2012).

Skeletal carbonates ($\delta^{13}\text{C}$)

$\delta^{13}\text{C}$ of skeletal carbonates were analysed on an 'Analytical Precision' sampler/mass spectrometer (de Groot, 2008). 1 mg samples of each powdered coral skeleton were sealed in vialtainers and flushed with helium. Phosphoric acid was injected through the septum in excess by the autosampler. The reaction was left at 70°C for 20 min to liberate CO₂ into the headspace. The resulting gas was analysed by the instrument's IRMS.

Dimethylated sulphur analyses

Approximately 1 mg of centrifuged tissue was diluted to 5 ml volume with MilliQ 18 Ω water with 1 ml 10 M NaOH and stored in 20 ml chromatography vials (Fisher Scientific) sealed with Pharma-Fix septa (Fisher Scientific), to hydrolyse DMSP into DMS. Samples were stored in the dark and transported back to the University of St Andrews for analysis. The sample headspace was analysed by direct injection using an SRI-8610C gas chromatograph (GC) (SRI Instruments UK) fitted with a 15 m 5.0U MXT-1 capillary column (N₂ carrier gas @ 8 psi, 45°C), and a sulphur-specific flame photometric detector (air pressure: 2 psi, H₂ pressure: 27 psi, 150°C).

Samples were then analysed for DMSO concentration, using the reductase enzyme method (Hatton *et al.*, 1994). Samples were purged of DMS with N₂ following addition of Tris-buffer and neutralization to pH 7.0. Where samples could not be analysed within 24 h of preparation, they were frozen (−20°C) until analysis. 2 ml of flavin mononucleotide solution was added to each vial and irradiated with 3 × 60 W bulbs for 1 h to catalyse the reaction of DMSO to DMS, following Hatton *et al.* (1994). Samples were left for 12 h to allow DMS equilibration in the vial headspace, before direct-injection GC analysis, as described above. All sample concentrations were quantified from DMSP standard calibration curves (DMSP standard from Research Plus Inc.). The limit of detection for both DMSP and DMSO samples was 1 µg S per 100 µl headspace injection; standard and sample precision was within 1%.

Statistical analyses

All statistical analyses and data manipulation were conducted in the programming language R (R-Core-Team, 2013). The minimum saturating irradiance (RLC[Ek]) and initial photosynthetic rate (RLC[alpha]) were calculated for each fragment by fitting rapid light curve (RLC) data to the equations of Jassby & Platt (1976) in the package Phytotools (Silsbe & Malkin, 2015). Maximum Relative Electron Transport Rate (RLC[rETRmax]) was calculated as RLC[Ek]*RLC[alpha]. As the δ¹³C skeletal value attains an equilibrium with the environment (McConnaughey *et al.*, 1997), and the difference to tissue δ¹³C represents a metabolic effect, we calculate a δ¹³C differential as δ¹³C tissue − δ¹³C skeleton. We rely on seawater δ¹³C DIC as an additional control for potential between site variation in δ¹³C sources, as it provides the basis for coral carbonate production (Allison *et al.*, 2014).

Linearity, normality, heteroscedasticity and influential outliers were assessed using residual plots. Statistical tests were not used to assess these as the large number of data points caused spurious rejection of assumptions with high *P* values associated with only small deviations. Tests are robust to the assumption of homogeneity of variance across groups because of balanced sample sizes between sites. Data remained untransformed to ensure fair comparisons between tests.

In turn, RLC[Ek], RLC[alpha], RLC[rETRmax], change in dissolved oxygen during incubation (ΔDO₂), tissue molar C:N, DMSO:DMSP, δ¹³C tissue differential, tissue δ¹⁵N, sediment δ¹⁵N, and seawater δ¹³C DIC were all fitted as the dependent variable of a linear model with depth as the independent variable, site as a grouping factor, and an interaction term. RLC[rETRmax], ΔDO₂, tissue molar C:N, δ¹³C tissue differential, tissue δ¹⁵N were also fitted in the same way against DMSO:DMSP. For the δ¹³C tissue differential, tissue molar C:N was included as a control variable to account for possible fluctuations in lipid content. These models show the physiological profile of *A. lamarcki* with depth at Utila, in terms of photosynthesis, heterotrophy, respiration and oxidative stress:

$$Y \sim (\text{Depth or DMSO : DMSP}) + \text{Site} + \text{interaction}$$

Additional models included:

$$\text{Tissue } \delta^{15}\text{N} \sim r\text{ETRmax} + \text{Site} + r\text{ETRmax} : \text{Site}$$

$$\delta^{13}\text{C differential} \sim \text{Tissue } \delta^{15}\text{N} + \text{Tissue molar C : N} \\ + \text{Site} + \text{Tissue } \delta^{15}\text{N} : \text{Site}$$

Statistically significant model elements were detected with heteroscedastically constant variance using ‘Anova(white.adjust = HC3)’ (Long & Ervin, 2000). The final data file can be found in the supplementary material (Supplementary 2).

Results

The changes in physiology recorded for *A. lamarcki* with increasing depth differ markedly between TMA and LB. A summary of ANCOVA results and model parameters are presented in Tables 1 and 2 respectively. Plots of environmental controls can be found in the supplementary material (Supplementary 3, Supplementary 4), as well as Residual plots (Supplementary 5). Residual plots revealed no systematic deviations from model assumptions. For analyses considering the δ¹³C tissue differential, molar C:N was included as an additional parameter to control for lipid content. Molar C:N did not vary with depth (*F* = 2.40, *P* = 0.12) or tissue δ¹⁵N (*F* = 8.94, *P* = 0.54).

During our sampling we did not encounter any intermediate, general colony-level, morphologies. Though morphological variation and change in growth form down depth gradients has been documented in some species of Scleractinia (Dustan, 1975; Amaral, 1994; Nir *et al.*, 2011; Goodbody-Gringley & Waletich, 2018), we observed only modest plasticity in growth form. At the extremes of *A. lamarcki*'s depth range, within a given site, there was a tendency toward smaller encrusting colonies. Plating forms were most common between ~20–55 m depth.

Physiological variation with depth

Three coral measures significantly varied with depth: δ¹⁵N as a signal of heterotrophy (*F* = 19.38, *P* < 0.001), δ¹³C differential as a signal of long-term photosynthetic activity (*F* = 5.53, *P* = 0.02), and RLC[rETRmax] as an instantaneous measure of potential photosynthetic capacity (*F* = 8.46, *P* = 0.004). ΔDO₂, molar tissue C:N, and DMSO:DMSP did not significantly vary with depth (Table 1). Mean values of tissue δ¹⁵N differed between sites for a given depth (*F* = 25.59, *P* < 0.001) – the mean at LB was 0.53‰ higher. Mean DMSO:DMSP values were 0.08 higher at TMA than LB (*F* = 4.23, *P* = 0.04). Differing slopes with depth were detected for RLC[rETRmax] and tissue δ¹⁵N (Figure 1) between sites (*F* = 8.87, *P* = 0.004; *F* = 14.13, *P* < 0.001, Table 1). We found potential photosynthetic capacity (RLC[rETRmax]) significantly declined with depth (Table 1), however, this appears to only be true at LB (Table 2, Figure 1). To further understand how photosynthetic profiles vary with depth, RLC[Ek] and RLC[alpha] were tested independently against depth, as RLC[rETRmax] is a composite of these two quantities. While RLC[alpha] significantly increased with depth, RLC[Ek] significantly decreased. Only RLC[Ek] returned a significant interaction term (Table 1), suggesting the observed differences in photosynthetic capacity with depth between the two sites were caused by differing RLC[Ek] values, i.e. the minimum saturating irradiance.

Environmental controls

No differences in environmental baselines were observed between the two sites. δ¹⁵N of sediment samples at LB and TMA (Supplementary 3) were collected as environmental baselines for comparison to changes in tissue values which may be affected by local enrichment (Heikoop *et al.*, 2000; Baker *et al.*, 2010). Both the environmental signal and tissue showed a significant relationship with depth (Table 1). No significant difference was detected in mean δ¹⁵N of sediments between sites, though parameter estimates indicated mean δ¹⁵N was slightly enriched at LB

Table 1. ANCOVA results: values are reported as they appeared in computer outputs

ANCOVA summaries	Sample size		Effect of X		Effect of site on means		Effect of site on slope		X variable
	N: LB	N: TMA	F	P	F	P	F	P	
RLC[Ek]	50	58	17.0856	0.00007251*	0.0135	0.90756	5.7756	0.01802*	Depth
RLC[alpha]	50	58	43.4559	1.835E-09*	0.3176	0.5743	2.1614	0.1445	Depth
RLC[rETRmax]	50	58	8.464	0.00443*	0.0199	0.888178	8.8711	0.003606*	Depth
DMSO:DMSO	44	44	1.7308	0.19158	4.2328	0.04248*	0.0505	0.82277	Depth
Incubation δDO_2	47	41	0.0064	0.9366	0.1543	0.6955	2.7145	0.103	Depth
Tissue molar C:N	48	54	0.0108	0.9176	0.0133	0.9083	2.5248	0.1153	Depth
$\delta^{13}\text{C}$ differential	48	54	5.5309	0.02068*	0.4084	0.52427	3.2029	0.0766	Depth
Tissue $\delta^{15}\text{N}$	48	54	19.378	0.00002711*	25.591	0.00001944*	14.128	0.0002889*	Depth
Sediment $\delta^{15}\text{N}$	14	24	8.1582	0.00726*	2.5446	0.11992	0.2265	0.6372	Depth
DIC seawater	4	18	10.9894	0.003851*	1.5271	0.23243	1.6271	0.218326	Depth
Tissue $\delta^{15}\text{N}$	48	54	1.786	0.1845	17.2591	0.00006928*	0.0972	0.7559	RLC[rETRmax]
$\delta^{13}\text{C}$ differential	48	54	0.3741	0.542172	4.9821	0.027888*	8.5822	0.004223*	Tissue $\delta^{15}\text{N}$
RLC[rETRmax]	44	44	0.0232	0.8794	0.3086	0.5799	1.2962	0.2579	DMSO:DMSP
Incubation δDO_2	43	33	0.0924	0.762	2.2564	0.1371	0.372	0.5437	DMSO:DMSP
Tissue molar C:N	44	44	4.1628	0.04429*	0.1721	0.67921	0.0833	0.77361	DMSO:DMSP
$\delta^{13}\text{C}$ differential	44	44	1.367	0.24545	3.9114	0.05105	1.0363	0.31145	DMSO:DMSP
Tissue $\delta^{15}\text{N}$	44	44	0.7734	0.3815	18.2509	4.839E-05*	0.5592	0.4566	DMSO:DMSP

P values <0.05 are in bold and followed by an *. LB, Site Little Bight; TMA, Site The Maze.

compared with TMA (+0.36‰). Though this was not statistically significant (Table 1), this value is close enough to the difference in mean levels between sites for tissue $\delta^{15}\text{N}$ that we conclude there is little biological meaning to the result. It is not believed that environmental patterns drive the relationship in the tissue since the gradients in tissue $\delta^{15}\text{N}$ with depth are in opposing directions, whereas the environmental signal is consistently positive (Table 2). $\delta^{13}\text{C}$ DIC of seawater (Supplementary 4) was collected and analysed as an environmental comparison to coral $\delta^{13}\text{C}$. Though DIC exhibits a statistically significant relationship with depth, this was in the opposite direction to the coral holobiont $\delta^{13}\text{C}$ measurement, and the effect size was at least an order of magnitude lower at each site (Table 2). Similarly to the sediment data, no statistically significant site differences were detected in $\delta^{13}\text{C}$ (Table 1); though LB had a mean $\delta^{13}\text{C}$ 0.05‰ higher than TMA. These results suggest the trends we see between sites result from physiological variation, and not differing environmental baselines between sites.

Relationships between photosynthesis (RLC[rETRmax] and $\delta^{13}\text{C}$), inferred heterotrophy ($\delta^{15}\text{N}$) and stress (DMSO:DMSP)

We detect two statistically supported relationships between DMSO:DMSP and other physiological variables. Firstly a reduction in tissue molar C:N with increasing DMSO:DMSP ($F = 4.16$, $P = 0.04$). Secondly an effect of site on mean levels of tissue bulk $\delta^{15}\text{N}$ ($F = 18.25$, $P < 0.001$), with higher $\delta^{15}\text{N}$ values for a given DMSO:DMSP at LB than TMA (Table 1). With $P = 0.051$, a notable effect of DMSO:DMSP on mean levels of the $\delta^{13}\text{C}$ tissue differential is identified, with higher $\delta^{13}\text{C}$ values at TMA than LB (Table 1).

A significant site and depth interaction for RLC[rETRmax] and for tissue $\delta^{15}\text{N}$ (Table 1, Figure 1) could be driven by two factors. Either, certain physiological relationships within the coral holobiont were not constant, or unmeasured sources of variation

were confounded differently with depth at the two sites. To aid interpretation, tissue $\delta^{15}\text{N}$ was plotted against RLC[rETRmax] (Figure 2) and statistically assessed, determining whether the physiological relationships remained constant between sites. Site affected mean values at the two sites, but only to the degree expected by the sediment control (Supplementary 3). There is no statistically supported relationship between RLC[rETRmax] and tissue $\delta^{15}\text{N}$ ($F = 1.79$, $P = 0.18$, Table 1), nor a significant interaction.

As there was, unexpectedly, no relationship between RLC [rETRmax] and tissue $\delta^{15}\text{N}$, we further explored the $\delta^{13}\text{C}$ differential result. When controlling for variability in molar C:N, the difference in slope between LB and TMA $\delta^{13}\text{C}$ with depth (Figure 1) was no longer statistically significant, $P = 0.08$ (Table 1). A relationship might be expected between photosynthetic parameters and the degree of heterotrophy, based on previous work (Alamaru *et al.*, 2009; Lesser *et al.*, 2010; Crandall *et al.*, 2016). We therefore plot the $\delta^{13}\text{C}$ differential against tissue $\delta^{15}\text{N}$ (Figure 2) and statistically assessed the relationships. Whilst there was no overall relationship between the two variables, a significant interaction term (Table 1) revealed opposing gradients at the two sites and differing group means (Table 2).

Variability of physiological measures between sites

Despite differences in physiology with depth between LB and TMA, the probability distributions of parameter values are broadly comparable (Figure 3). If the physiological parameters in Figure 3 were linearly correlated with depth, we would expect the probability distributions to reflect the sampling effort with depth. The distributions at both sites return a modal value in close agreement and are more tightly grouped around this value than expected with sampling effort, despite sampling different depth ranges at the two sites. The exception is a shift in DMSO:DMSP between the two sites, consistent with the

Table 2. Model parameters. values are reported as they appeared in computer outputs

Model summaries	Little bight		The maze		Adjusted R^2	Residuals	X variable	Interpretation
	Intercept	Slope	Intercept	Slope				
RLC[Ek]	206.227352	-2.692050	143.694792	-0.879897	0.1705	N	Depth	Minimum saturating irradiance
RLC[alpha]	0.492716055	0.001374574	0.449357211	0.002833639	0.228	M	Depth	Initial photosynthetic rate
RLC[rETRmax]	100.220204	-1.204346	67.201354	-0.175732	0.1412	A	Depth	Photosynthetic capacity (relative electron transport rate)
DMSP:DMSO	0.75419628	-0.002717019	0.816521507	-0.001934149	0.01403	Q	Depth	Inferred oxidative stress
Incubation δDO_2	-17.9271223	0.3868667	-64.6352683	-0.7049168	0.0003409	D	Depth	Net photosynthesis during dark trials
Tissue molar C:N	13.6679714	0.0446042	8.9962262	-0.0825296	0.006482	E	Depth	Holobiont condition
$\delta^{13}\text{C}$ differential	-15.88822	-0.01171	-13.94745	-0.08405	0.1926	C	Depth	Long-term photosynthetic signal
Tissue $\delta^{15}\text{N}$	1.63560878	0.03637871	2.29028497	-0.00204339	0.2585	B	Depth	Inferred trophic level
Sediment $\delta^{15}\text{N}$	2.86968	0.7132	2.40521	0.69883	0.2104	K	Depth	Environmental control
DIC seawater	0.88	8.29E-19	0.6542	0.005055	0.4287	L	Depth	Environmental control
Tissue d^{15}N	3.000773	-0.004688	2.9671088	-0.007505	0.1366	O	RLC[rETRmax]	Investigating site differences
$\delta^{13}\text{C}$ differential	-14.37608	-0.97474	-20.32498	1.10782	0.1584	P	Tissue $\delta^{15}\text{N}$	Investigating site differences
RLC[rETRmax]	53.35772	16.19293	66.32352	-7.45428	0.01279	F	DMSO:DMSP	Photosynthetic capacity (relative electron transport rate)
Incubation δDO_2	-6.487366	-3.052744	-13.446896	30.751496	0.007288	I	DMSO:DMSP	Net photosynthesis during dark trials
Tissue molar C:N	17.385736	-3.462559	18.745543	-4.712544	3.32E-05	J	DMSO:DMSP	Holobiont condition
$\delta^{13}\text{C}$ differential	-13.212548	-2.262587	-15.850777	-4.685545	0.05017	H	DMSO:DMSP	Long-term photosynthetic signal
Tissue $\delta^{15}\text{N}$	2.7326381	-0.1110724	2.5391774	-0.5638523	0.0002416	G	DMSO:DMSP	Inferred trophic level

References to the residual plots in supplementary information for each model are under column 'Residuals'. 'Interpretation' is a brief explanation of what the model represents. LB, Site Little Bight; TMA, Site The Maze.

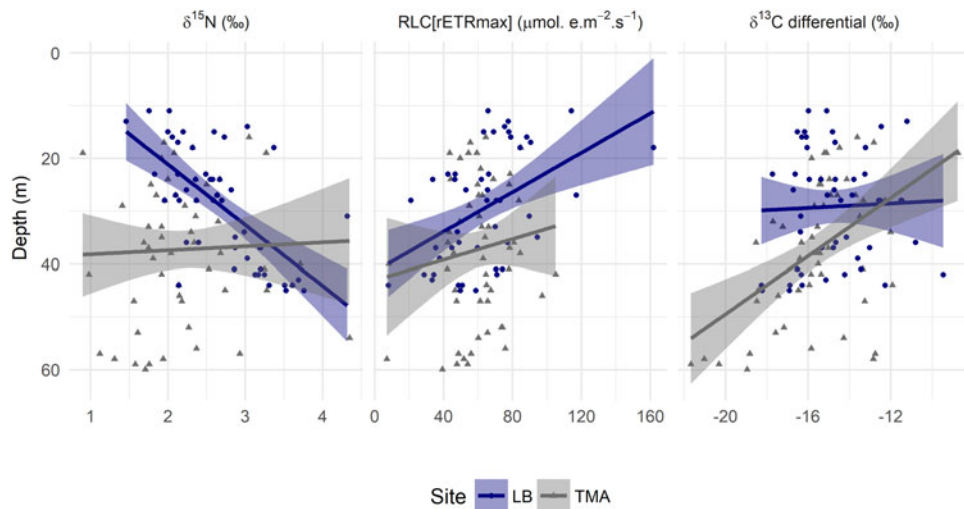


Fig. 1. Principal physiological relationships of *Agaricia lamarcki* with depth across two sites: Linear models of bulk tissue $\delta^{15}\text{N}$, RLC[rETRmax] and the $\delta^{13}\text{C}$ differential against depth. Shaded areas are the 0.95 confidence interval. Statistical assessment and model parameters can be found in Tables 1 and 2. LB, Site Little Bight; TMA, Site The Maze.

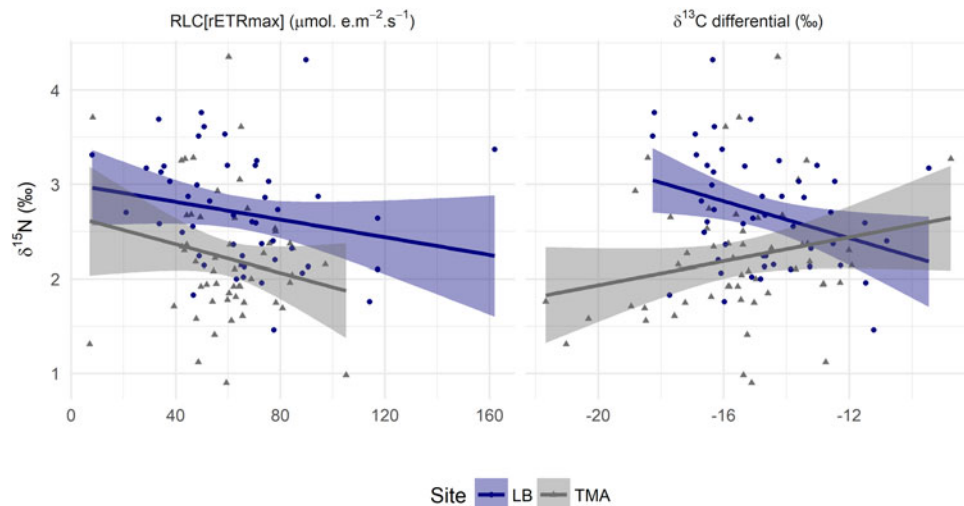


Fig. 2. Variation in inferred trophic level by photosynthetic capacity and inferred, *in situ*, photosynthetic activity of *Agaricia lamarcki* across two sites: Linear model of $\delta^{15}\text{N}$ by RLC[rETRmax]. Linear model of $\delta^{13}\text{C}$ differential by bulk tissue $\delta^{15}\text{N}$. Shaded areas are the 0.95 confidence interval. Statistical assessment and model parameters can be found in Tables 1 and 2. LB, Site Little Bight; TMA, Site The Maze.

differences in mean levels detected by linear models (Table 1). The probability distribution for TMA is consistently narrower than for LB, despite TMA being sampled over a larger depth range which we would expect to necessitate greater physiological variation.

Discussion

Agaricia lamarcki expresses site-specific physiological profiles with depth

This study aimed to assess the constancy of physiological patterns with depth between sites in the depth-generalist mesophotic coral, *Agaricia lamarcki*. We found clear site-specific trends, both in terms of PAM fluorometry and stable isotope analyses. At LB, *A. lamarcki* exhibited a reduction in potential photosynthetic capacity and an increase in heterotrophic feeding with depth (Figure 1). These patterns were absent at TMA, despite a wider vertical depth range. These observations highlight the variability of scleractinian physiology, and the importance of taking into

consideration local/regional scale variation when attempting to generalize biological response. We have shown that the same species of coral will not necessarily behave in the same way down a depth gradient in different locations. Depth alone may therefore be an inappropriate proxy for physiological change through the mesophotic zone. We should instead consider more explicitly the role of the underwater light field when explaining mesophotic coral physiology (Lesser *et al.*, 2018), and how this can interact with reef topography (Muir *et al.*, 2018; Kramer *et al.*, 2019).

The deepest colonies of A. lamarcki can be comparable to those more shallow

In addition to the trends in tissue $\delta^{15}\text{N}$ and RLC[rETRmax], there were no detected trends in respiration (as inferred from ΔDO_2), and no trend in the molar C:N ratio (Table 1, Supplementary 5). The lack of trend in respiration and molar C:N is of interest when taking into account the significant reduction in RLC[Ek] with depth (Table 2), which underpins a reduction in potential photosynthetic capacity (Figure 1). The change in RLC[Ek] clearly

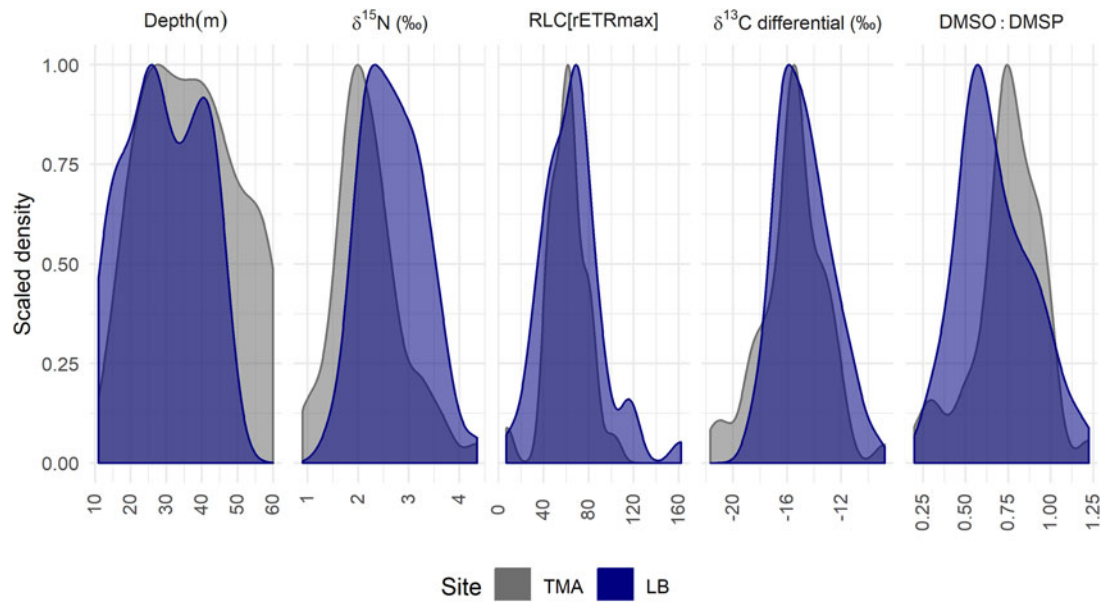


Fig. 3. Probability distributions of select parameter values: The height of the curve indicates the relative probability of a particular parameter value. Each curve is scaled so 1 reflects the modal value within a site, the area under each curve sums to a probability of 1. The distributions from left to right show the sampled colonies with depth, values of bulk tissue $\delta^{15}\text{N}$, RLC[rETRmax], $\delta^{13}\text{C}$ differential and DMSO:DMSP. If physiological parameters were correlated linearly with depth, we would expect distributions to be similar to those shown for sample collections depths. LB, Site Little Bight, TMA, Site The Maze.

indicates that deeper *A. lamarcki* colonies are acclimated to lower light levels; they do not exhibit lower fat stores or rates of energy consumption at the light levels used in this study. This leads us to believe that the potential adaptation of deeper colonies may not prevent connectivity between shallow and mesophotic reefs and may permit a deep-water refuge for *A. lamarcki* at this location. This is supported by the lack of an observed effect of depth on the cellular oxidative stress indicator DMSO:DMSP, and by no impact of collection site on the survival of the same colonies sampled here during a transplant experiment (Laverick & Rogers, 2018). A similar situation has been noted for *E. paradivisa* in the Red Sea (Eyal *et al.*, 2015). ΔDO_2 in the dark, however, approximates basal metabolic rate which is expected to be largely constant (Suarez *et al.*, 2004; Makarieva *et al.*, 2008). *In situ* measurements of net-photosynthesis year round are necessary to better understand the importance of respiration in balancing energy budgets with increasing depth.

Interpreting our stable isotope data, with respect to photosynthetic activity, comes with caveats. Coral growth rates can vary with increasing depth (Baker & Weber, 1975), and this in turn can leave isotopic signals (Patzold, 1984). Further, coral growth rates can vary with light exposure, independent of changes in photosynthesis (Eyal *et al.*, 2019). Growth signals can also correlate with light exposure in skeletal carbon fractionation (Shimamura *et al.*, 2008). Further studies which could quantify the variation in *A. lamarcki* growth rates with depth would be valuable. This would allow the isotopic signatures of growth and photosynthesis to be disentangled but would also be helpful for demographic studies. For $\delta^{15}\text{N}$, symbiodinium growth rate does not affect nitrogen isotope fractionation (Muscatine & Kaplan, 1994).

The observed negative relationship between C:N and DMSO:DMSP supports the role of tissue C:N as an indicator of holobiont health (Szmant & Gassman, 1990) and further supports the use of DMSO:DMSP as an indicator of cellular stress (Husband & Kiene, 2007; McFarlin & Alber, 2013). Between-site differences in mean DMSO:DMSP support the hypothesis that spatial variation in environmental conditions is impacting the local-scale physiology of *A. lamarcki*.

Physiological profiles are coincident with differences in ecological patterns

Our findings also reveal a connection between physiological parameters and ecological patterns. If we interpret the difference between mean tissue $\delta^{15}\text{N}$ at the two sites (Figure 1, Table 2) as resulting from differing environmental baselines (Supplementary 3, Table 2), then there was no difference in the mean value of any physiological parameter between the two sites, except DMSO:DMSP. This observation is despite the larger depth range at TMA. Significant interaction terms for tissue $\delta^{15}\text{N}$ and RLC[rETRmax] show that it is the rates of change with depth which vary, such that the same physiological limits are reached for these parameters. In fact, the minimum saturating irradiance (RLC[Ek]) reduces at a rate three times faster at LB than TMA with depth, while RLC[alpha] increases at more than twice the rate with depth at TMA ($0.28\% \text{ m}^{-1}$) than LB ($0.13\% \text{ m}^{-1}$), although this relationship was too noisy to return a statistically significant interaction term. Both quantities are considered key photoadaptations with increasing depth in coral (Chalker *et al.*, 1983). We expect corals from low light environments to have higher alpha values, and lower Ek values, as they optimize themselves to quickly capture the small amount of light available. Although we are able to detect variation in the rates of photoadaptation with depth, the use of RLCs prevents us from distinguishing between photosynthetic characteristics and bio-optical properties as the causative factor in these observations.

These findings do suggest that depth ranges and physiological change are related. If site-specific environmental conditions are the root cause of differing distributions for coral taxa between sites (Anthony & Hoegh-Guldberg, 2003), then we may have an explanation for observations of mesophotic taxa at 'unusual' depths (Muir & Wallace, 2015; Laverick *et al.*, 2017). Increasingly in mesophotic ecology there are calls for a biologically informed, rather than depth-lineated, definition of mesophotic reefs (Laverick *et al.*, 2016; Loya *et al.*, 2016; Semmler *et al.*, 2016; Lesser *et al.*, 2018), as intended (Baker *et al.*, 2016a). Coral species typical of the mesophotic zone are known to prefer shaded microhabitats at shallower depths (Muir *et al.*, 2018; Kramer *et al.*, 2019). Meanwhile, the potential role the underwater light field could play in controlling the distribution of mesophotic reefs has been

highlighted through simulations of varying reef structure (Lesser *et al.*, 2018). Lesser *et al.* suggested that a more nuanced definition of MCEs may be in reach if the light field can be connected to the intrinsic properties of coral communities. We have shown how physiological patterns between sites could translate into differing depth distributions for *A. lamarcki* on Utila. We now suggest that considering the interaction between physiology and the light field, at a community level, could allow us to expand the concept of mesophotic habitats.

Agaricia lamarcki appears to be a mixotroph

Previous studies have attempted to interpret physiological data and claim particular species are primarily heterotrophic or photoautotrophic (Lesser *et al.*, 2010; Crandall *et al.*, 2016). Specifically *A. lamarcki* has been previously identified as a heterotrophic coral (Crandall *et al.*, 2016). Our high degree of replication within sites, in conjunction with a cross-site comparison, provides robust evidence for notable mixotrophy in *A. lamarcki*. Our trends in bulk tissue $\delta^{15}\text{N}$ and $\delta^{13}\text{C}$ at LB indicate heterotrophy (Figure 1), in agreement with previously published research (Crandall *et al.*, 2016). The trends detected at TMA, however, are more similar to those reported by others for *Montastraea cavernosa* (Lesser *et al.*, 2010; Crandall *et al.*, 2016). Though we do not have the compound-specific stable isotope analysis of sterols used by Crandall *et al.* (2016), we do detect a decrease in $\delta^{13}\text{C}$ without a commensurate increase in $\delta^{15}\text{N}$. This suggests a primarily photosynthetic strategy at TMA. Further, the statistically significant trends in RLC[Ek] and RLC[alpha] with depth indicate photoadaptation (driven by changes in photosynthetic characteristics and/or bio-optical properties) is occurring. As RLC[alpha] increases at twice the rate with depth at TMA, and over a larger depth gradient, it may be that photoadaptation is sufficient to maintain an autotrophic strategy at this location, but not at LB. This difference in strategy between the two sites is interesting, as we observed no differences by site in the relationship between photosynthetic capacity and tissue $\delta^{15}\text{N}$ (Figure 2). Site differences in the change in environmental conditions by depth may therefore have been responsible for the apparent switch in hetero/autotrophic strategy with depth between the two sites.

An interesting extra area of research for mesophotic coral physiology concerns the seasonal fluctuations in energy availability. In the Red Sea net O_2 production in *S. pistillata* varies through the year (Nir *et al.*, 2014), indicating a shift in the relative contributions of heterotrophy and photosynthesis over time. For *A. lamarcki* in the US Virgin Islands different temporal trends in energy content were detected with increasing depth. In contrast to corals at 25 m, corals at 63 m were starved in July–September, and compensate through November–April (Brandtneris *et al.*, 2016). It may be possible that the site-specific conditions of TMA on the north, and LB on the south, side of Utila may come from seasonal asynchrony, as opposed to constant differences. Only time series studies at depth, which are highly unusual on MCEs, will be able to help us understand how energy budgets are balanced across the course of a year.

Exploiting available microhabitat may explain physiological consistency at the maze, a hypothesis

In comparison to LB, very few physiological changes with depth were observed at TMA. This was despite colonies being collected across a 44 m depth range and comparable modal parameter values between both sites (Figure 3). One potential explanation is that the topography of TMA is more complex than the gentle slope of LB, affording more light-equivalent microhabitats for colonies to exploit (Brakel, 1979). Photosynthetic capacity in Scleractinia has been shown to correlate with the light


environment of microhabitats (Anthony & Hoegh-Guldberg, 2003; Bessell-Browne *et al.*, 2017). Given the rate of light attenuation with depth, we may expect the relative difference in light intensity between microhabitats (e.g. illuminated vs shaded) to be greater at shallower depths than deeper, and we do not expect mesophotic reefs to be exposed to a higher light intensity than shallower reefs. Given a random distribution of coral colonies across these microhabitats and *in situ* acclimation, we would expect similar heteroscedasticity in photosynthetic capacity. Our residual plots revealed no notable deviation from the assumption of homoscedasticity in photosynthetic capacity with depth (Supplementary 5A).

Similarly microhabitats with low flow rates, and therefore food availability, have been shown to impact the growth of *Agaricia tenuifolia* in shallow waters down a depth gradient (Sebens *et al.*, 2003). Low flow rates in the mesophotic favour ciliary mucus feeders such as *A. lamarcki* in general (Sebens & Johnson, 1991). Varying flow rates between microhabitats at TMA may permit a more constant heterotrophic contribution to the energy budget with depth (Figure 1).

Further, Figure 3 shows the probability distributions of the parameters with the greatest between site differences, as well as the depth distribution of sampled colonies for a null comparison. In all cases, the colonies at TMA have a tighter distribution around a modal value, despite being sampled over a larger depth range than at LB. Figure 3 shows a tighter distribution at TMA in terms of DMSO:DMSP, suggesting lower inter-colony variability in oxidative stress, and so potentially irradiance. This could also in part be explained by higher variability in irradiance levels at LB as a result of the south-facing nature of the site, in comparison to TMA on the north shore of Utila. Differing site means of DMSO:DMSP with depth may also indicate maintained higher irradiance levels at TMA (Table 1), corroborated by lower rates of change in RLC[Ek] at TMA with depth. This suggests *A. lamarcki* is better able to exist in a sub-set of preferred, stable, microhabitats at TMA.

Consideration of environmental conditions is already being used to predict the occurrence of mesophotic taxa in the Hawaiian archipelago (Costa *et al.*, 2015). Environmental data (e.g. temperature, irradiance, sedimentation, turbidity) and holobiont genetic information (e.g. symbiont type, gene regulation) may have provided a mechanism to explain the differences we observed. Because of an absence of environmental measures, we are unable to explain the cause of documented pattern. We do, however, make some suggestions for further research. At TMA, appropriate microhabitats appear to extend deeper than at LB, increasing the vertical range of *A. lamarcki* and mitigating physiological response to depth, at this location. This leads us to hypothesize that sites with greater topographical complexity are more likely to act as depth refuges, though this will require explicit testing across other species. Such sites begin to break the correlation of environmental conditions with depth (Brakel, 1979), allowing suitable microhabitats to exist below surface pressures (Bridge *et al.*, 2013). We have found that site-specific conditions may influence physiology to a greater degree than depth for *A. lamarcki*. Future physiology studies should try to record the light environment that colonies are located in, preferably with temporal variation, and relate this to substrate slope and shading.

Supplementary material. The supplementary material for this article can be found at <https://doi.org/10.1017/S0025315419000547>

Author ORCID.  Jack H. Laverick, 0000-0001-8829-2084.

Acknowledgements. The author would like to thank Grace C. Young for dive time, especially at TMA, Andrea P. Izaguirre-Luque from BICA for help with sample preparation in the field and 'coral-flossing', and Dominic

Andradi-Brown for sediment aliquots. The staff of Operation Wallacea at the Coral View research station, the Bay Islands Conservation Association, and the Natural Environment Research Council Life Sciences Mass Spectrometry Facility provided invaluable logistical and technical support. A final thank you to the reviewers who helped improve this manuscript.

Financial support. The authors would like to thank the Royal Geographical Society (Ralph-Brown Award), the Zoological Society of London (EDB Expeditions fund), the Oxford University Expeditions Council, Oxford University Press (John-Fell fund), the Natural Environment Research Council (NE/L002612/1; EK258-13/15), Merton College Oxford and Operation Wallacea for funding. TG is supported by a 7th Century University scholarship. Fieldwork was completed when HB was in receipt of a Marine Alliance for Science and Technology for Scotland (MASTS) Research Fellowship. DMSO analyses were supported by a MASTS Small Grant awarded to TG. MASTS is funded by the Scottish Funding Council (grant reference HR09011) and contributing institutions. We thank the Natural Environment Research Council (NERC) Field Spectroscopy Facility for loan of the Diving-PAM instrument.

References

- Alamaru A, Loya Y, Brokovich E, Yam R and Shemesh A (2009) Carbon and nitrogen utilization in two species of Red Sea corals along a depth gradient: insights from stable isotope analysis of total organic material and lipids. *Geochimica et Cosmochimica Acta* **73**, 53333–55342.
- Allison N, Cohen I, Finch AA, Erez J and Tudhope AW (2014) Corals concentrate dissolved inorganic carbon to facilitate calcification. *Nature Communications* **5**, 5741.
- Amaral FD (1994) Morphological variation in the reef coral in Brazil. *Coral Reefs* **13**, 113–117.
- Anthony KRN and Hoegh-Guldberg O (2003) Variation in coral photosynthesis, respiration and growth characteristics in contrasting light microhabitats: an analogue to plants in forest gaps and understoreys? *Functional Ecology* **17**, 246–259.
- Baker DM, Jordán-Dahlgren E, Maldonado MA and Harvell CD (2010) Sea fan corals provide a stable isotope baseline for assessing sewage pollution in the Mexican Caribbean. *Limnology and Oceanography* **55**, 2139–2149.
- Baker E, Puglise KA, Colin PL, Harris PT, Kahng SE, Rooney JJ, Sherman C, Slattery M and Spalding HL (2016a) What are Mesophotic Coral Ecosystems? In *Mesophotic Coral Ecosystems – A Life Boat for Coral Reefs?* Nairobi: United Nations Environment Programme, pp. 11–19.
- Baker EK, Puglise KA and Harris PT (2016b) *Mesophotic Coral Ecosystems – A Life Boat for Coral Reefs?* Nairobi: United Nations Environment Programme, GRID-ARENDAL.
- Baker PA and Weber JN (1975) Coral growth rate: variation with depth. *Earth and Planetary Science Letters* **27**, 57–61.
- Bessell-Browne P, Negri AP, Fisher R, Clode PL, Duckworth A and Jones R (2017) Impacts of turbidity on corals: the relative importance of light limitation and suspended sediments. *Marine Pollution Bulletin* **117**, 161–170.
- Bongaerts P, Riginos C, Hay KB, van Oppen MJ, Hoegh-Guldberg O and Dove S (2011) Adaptive divergence in a scleractinian coral: physiological adaptation of *Seriatopora hystrix* to shallow and deep reef habitats. *BMC Evolutionary Biology* **11**, 303.
- Bongaerts P, Carmichael M, Hay KB, Tonk L, Frade PR and Hoegh-Guldberg O (2015) Prevalent endosymbiont zonation shapes the depth distributions of scleractinian coral species. *Royal Society Open Science* **2**, 140297.
- Borell EM, Pettay DT, Steinke M, Warner M and Fine M (2016) Symbiosis-specific changes in dimethylsulphoniopropionate concentrations in *Stylophora pistillata* along a depth gradient. *Coral Reefs* **35**, 1383–1392.
- Brakel WH (1979) Small-scale spatial variation in light available to coral reef benthos: quantum irradiance measurements from a Jamaican reef. *Bulletin of Marine Science* **29**, 406–413.
- Brandtneris VW, Brandt M, Glynn PW, Gyory J and Smith TB (2016) Seasonal variability in calorimetric energy content of two Caribbean mesophotic corals. *PLoS ONE* **11**, 1–19.
- Bridge TCL, Hughes TP, Guinotte JM and Bongaerts P (2013) Call to protect coral reefs. *Nature Climate Change* **3**, 528–530.
- Brokovich E, Ayalon I, Einbinder S, Segev N, Shaked Y, Genin A, Kark S and Kiflawi M (2010) Grazing pressure on coral reefs decreases across a wide depth gradient in the Gulf of Aqaba, Red Sea. *Marine Ecology Progress Series* **399**, 69–80.
- Burdett H, Carruthers M, Donohue P, Wicks L, Hennige S, Roberts J and Kamenos N (2014) Effects of high temperature and CO₂ on intracellular DMSP in the cold-water coral *Lophelia pertusa*. *Marine Biology* **161**, 1499–1506.
- Chalker BE, Dunlap WC and Oliver JK (1983) Bathymetric adaptations of reef-building corals at Davies Reef, Great Barrier Reef, Australia. II. Light saturation curves for photosynthesis and respiration. *Journal of Experimental Marine Biology and Ecology* **73**, 37–56.
- Cohen I and Dubinsky Z (2015) Long term photoacclimation responses of the coral *Stylophora pistillata* to reciprocal deep to shallow transplantation: photosynthesis and calcification. *Frontiers in Marine Science* **2**, 45.
- Costa B, Kendall MS, Parrish FA, Rooney J, Boland RC, Chow M, Lecky J, Montgomery A and Spalding H (2015) Identifying suitable locations for mesophotic hard corals offshore of Maui, Hawai'i. *PLoS ONE* **10**, 1–24.
- Crandall JB, Teece MA, Estes BA, Manfrino C and Ciesla JH (2016) Nutrient acquisition strategies in mesophotic hard corals using compound specific stable isotope analysis of sterols. *Journal of Experimental Marine Biology and Ecology* **474**, 133–141.
- Davies PS (1980) Respiration in some Atlantic reef corals in relation to vertical distribution and growth form. *Biological Bulletin* **158**, 187–194.
- de Groot PA (ed.) (2008) *Handbook of Stable Isotope Analytical Techniques*. Amsterdam: Elsevier.
- Downs C (2011) Protocol for collection of coral tissue, vessel bottom paint and sediments. Technical Report. WWF, 1–16.
- Dustan P (1975) Growth and form in the reef-building coral *Montastrea annularis*. *Marine Biology* **33**, 101–107.
- Einbinder S, Mass T, Brokovich E, Dubinsky Z, Erez J and Tchernov D (2009) Changes in morphology and diet of the coral *Stylophora pistillata* along a depth gradient. *Marine Ecology Progress Series* **381**, 167–174.
- Einbinder S, Gruber DF, Salomon E, Liran O, Keren N and Tchernov D (2016) Novel adaptive photosynthetic characteristics of mesophotic symbiotic microalgae within the reef-building coral, *Stylophora pistillata*. *Frontiers in Marine Science* **3**, 195.
- Enríquez S, Méndez ER, Hoegh-Guldberg O and Iglesias-Prieto R (2017) Key functional role of the optical properties of coral skeletons in coral ecology and evolution. *Proceedings of the Royal Society B: Biological Sciences* **284**, 20161667.
- Eyal G, Eyal-Shaham L, Cohen I, Tamir R, Ben-Zvi O, Sinniger F and Loya Y (2015) *Euphyllia paradivisa*, a successful mesophotic coral in the northern Gulf of Eilat/Aqaba, Red Sea. *Coral Reefs* **35**, 91–102.
- Eyal G, Cohen I, Eyal-Shaham L, Ben-Zvi O, Tikochinski Y and Loya Y (2019) Photoacclimation and induction of light-enhanced calcification in the mesophotic coral *Euphyllia paradivisa*. *Royal Society Open Science* **6**, 180527.
- Feldman B, Shlesinger T and Loya Y (2017) Mesophotic coral-reef environments depress the reproduction of the coral *Paramontastraea peresi* in the Red Sea. *Coral Reefs* **37**, 1–14.
- Fourle F, Martineau F, Seris M and Lécuyer C (2014) Simultaneous N, C, S stable isotope analyses using a new purge and trap elemental analyzer and an isotope ratio mass spectrometer. *Rapid Communications in Mass Spectrometry* **28**, 2587–2594.
- Goodbody-Gringley G and Waletich J (2018) Morphological plasticity of the depth generalist coral, *Montastraea cavernosa*, on mesophotic reefs in Bermuda. *Ecology* **99**, 1688–1690.
- Graus RR and MacIntyre IG (1982) Variation in growth forms of the reef coral *Montastrea annularis* (Ellis and Solander): a quantitative evaluation of growth response to light distribution using computer simulation. *Smithsonian Contributions to the Marine Sciences* **12**, 441–464.
- Grottoli AG, Warner ME, Levas SJ, Aschaffenburg MD, Schoepf V, McGinley M, Baumann J and Matsui Y (2014) The cumulative impact of annual coral bleaching can turn some coral species winners into losers. *Global Change Biology* **20**, 3823–3833.
- Hatcher BG (1988) Coral reef primary productivity: a beggar's banquet. *Trends in Ecology and Evolution* **3**, 106–111.
- Hatton AD, Malin G, McEwan A and Liss P (1994) Determination of dimethyl sulfoxide in aqueous solution by an enzyme-linked method. *Analytical Chemistry* **4093**, 4096.
- Heikoop JM, Risk MJ, Lazier AV, Edinger EN, Jompa J, Limmon GV, Dunn JJ, Browne DR and Schwarcz HP (2000) Nitrogen-15 signals of anthropogenic nutrient loading in reef corals. *Marine Pollution Bulletin* **40**, 628–636.

- Hennige S, Smith D, Perkins R, Consalvey M, Paterson D and Suggett D (2008) Photoacclimation, growth and distribution of massive coral species in clear and turbid waters. *Marine Ecology Progress Series* **369**, 77–88.
- Humann P and Deloach N (2013) *Reef Coral Identification: Florida, Caribbean, Bahamas*, Third Edition. Jacksonville, FL: New World Publications.
- Husband JD and Kiene RP (2007) Occurrence of dimethylsulfoxide in leaves, stems, and roots of *Spartina alterniflora*. *Wetlands* **27**, 224–229.
- Jassby AD and Platt T (1976) Mathematical formulation of the relationship between photosynthesis and light for phytoplankton. *Limnology and Oceanography* **21**, 540–547.
- Johannes RE and Wiebe WJ (1970) Method for determination of coral tissues biomass and composition. *Limnology and Oceanography* **15**, 822–824.
- Juneau P, Green BR and Harrison PJ (2005) Simulation of Pulse-Amplitude-Modulated (PAM) fluorescence: limitations of some PAM-parameters in studying environmental stress effects. *Photosynthetica* **43**, 75–83.
- Kahng SE, Hochberg EJ, Apprill A, Wagner D, Luck DG, Perez D and Bidigare RR (2012) Efficient light harvesting in deep-water zooxanthellate corals. *Marine Ecology Progress Series* **455**, 65–77.
- Kahng SE, Copus JM and Wagner D (2014) Recent advances in the ecology of mesophotic coral ecosystems (MCEs). *Current Opinion in Environmental Sustainability* **7**, 72–81.
- Kramer N, Eyal G, Tamir R and Loya Y (2019) Upper mesophotic depths in the coral reefs of Eilat, Red Sea, offer suitable refuge grounds for coral settlement. *Scientific Reports* **9**, 2263.
- Laverick JH and Rogers AD (2018) Experimental evidence for reduced mortality of *Agaricia lamarcki* on a mesophotic reef. *Marine Environmental Research* **134**, 37–43.
- Laverick JH, Andradi-Brown DA, Exton DA, Bongaerts P, Bridge TCL, Lesser MP, Pyle RL, Slattery M, Wagner D and Rogers AD (2016) To what extent do mesophotic coral ecosystems and shallow reefs share species of conservation interest? *Environmental Evidence* **5**, 16.
- Laverick JH, Andradi-Brown DA and Rogers AD (2017) Using light-dependent scleractinia to define the upper boundary of mesophotic coral ecosystems on the reefs of Utila, Honduras. *PLoS ONE* **12**, e0183075.
- Lesser MP, Slattery M and Leichter JJ (2009) Ecology of mesophotic coral reefs. *Journal of Experimental Marine Biology and Ecology* **375**, 1–8.
- Lesser MP, Slattery M, Stat M, Ojimi M, Gates RD and Grottole A (2010) Photoacclimatization by the coral *Montastraea cavernosa* in the mesophotic zone: light, food, and genetics. *Ecology* **91**, 990–1003.
- Lesser MP, Mazel C, Phinney D, Yentsch CS and Mazell C (2014) Corals light absorption and utilization by colonies of the congeneric *Montastraea faveolata* and *Montastraea cavernosa*. *American Society of Limnology and Oceanography* **45**, 76–86.
- Lesser MP, Slattery M and Mobley CD (2018) Biodiversity and functional ecology of mesophotic coral reefs. *Annual Review of Ecology, Evolution, and Systematics* **49**, 49–71.
- Long JS and Ervin LH (2000) Using heteroscedasticity consistent standard errors in the linear regression model. *American Statistician* **54**, 217–224.
- Loya Y, Eyal G, Treibitz T, Lesser MP and Appeldoorn R (2016) Theme section on mesophotic coral ecosystems: advances in knowledge and future perspectives. *Coral Reefs* **35**, 1–9.
- Makariev AM, Gorshkov VG, Li B-L, Chown SL, Reich PB and Gavrilov VM (2008) Mean mass-specific metabolic rates are strikingly similar across life's major domains: evidence for life's metabolic optimum. *Proceedings of the National Academy of Sciences USA* **105**, 16994–9.
- McConnaughey TA, Burdett J, Whelan JF and Paull CK (1997) Isotopes in biological carbonates: respiration and photosynthesis. *Geochimica et Cosmochimica Acta* **61**, 611–622.
- McFarlin CR and Alber M (2013) Foliar DMSO:DMSR ratio and metal content as indicators of stress in *Spartina alterniflora*. *Marine Ecology Progress Series* **474**, 1–13.
- Muir PR and Wallace CC (2015) A rare 'deep-water' coral assemblage in a shallow lagoon in Micronesia. *Marine Biodiversity* **46**, 3.
- Muir PR, Wallace CC, Pichon M and Bongaerts P (2018) High species richness and lineage diversity of reef corals in the mesophotic zone. *Proceedings of the Royal Society B: Biological Sciences* **285**, 20181987.
- Muscatine L and Kaplan IR (1994) Resource partitioning by reef corals as determined from stable isotope composition. II. $\delta^{15}\text{N}$ of zooxanthellae and animal tissue vs depth. *Pacific Science* **48**, 304–312.
- Muscatine L, Porter JW and Kaplan IR (1989) Resource partitioning by reef corals as from stable isotope composition. I. $\delta^{13}\text{C}$ of zooxanthellae and animal tissue vs depth determined. *Marine Biology* **100**, 85–193.
- Newton J (2010) Continuous-flow isotope ratio mass spectrometry with an elemental analyzer: oxidative approaches for carbon and nitrogen isotopes. In Beauchemin D and Matthews D (eds) *Elemental and Isotope Ratio Mass Spectrometry. Series: The Encyclopedia of Mass Spectrometry*. Amsterdam: Elsevier, pp. 759–764.
- Nir O, Gruber DF, Einbinder S, Kark S and Tchernov D (2011) Changes in scleractinian coral *Seriatopora hystrix* morphology and its endocellular Symbiodinium characteristics along a bathymetric gradient from shallow to mesophotic reef. *Coral Reefs* **30**, 1089–1100.
- Nir O, Gruber DF, Shemesh E, Glasser E and Tchernov D (2014) Seasonal mesophotic coral bleaching of *Stylophora pistillata* in the Northern Red Sea. *PLoS ONE* **9**, 1–8.
- Palardy JE, Grottole AG and Matthews KA (2005) Effects of upwelling, depth, morphology and polyp size on feeding in three species of Panamanian corals. *Marine Ecology Progress Series* **300**, 79–89.
- Patzold J (1984) Growth rhythms recorded in stable isotopes and density bands in the reef coral *Porites lobata* (Cebu, Philippines). *Coral Reefs* **3**, 87–90.
- Peterson BJ and Fry B (1987) Stable isotopes in ecosystem studies. *Annual Review of Ecology and Systematics* **18**, 293–320.
- Puglise K, Hinderstein L, Marr J, Dowgiallo M and Martinez F (2009) *Mesophotic Coral Ecosystems Research Strategy: International Workshop to Prioritize Research and Management Needs for Mesophotic Coral Ecosystems*, Jupiter, Florida, 12–15 July 2008. Silver Spring, MD: NOAA National Center for Sponsored Coastal Ocean Research and Office of Ocean Exploration and Research, NOAA Undersea Research Program. NOAA Technical Memorandum NOS NCCOS 98 and OAR OER 2. 24 pp.
- Qi H, Coplen TB, Geilmann H, Brand WA and Böhlke JK (2003) Two new organic reference materials for $\delta^{13}\text{C}$ and $\delta^{15}\text{N}$ measurements and a new value for the $\delta^{13}\text{C}$ of NBS 22 oil. *Rapid Communications in Mass Spectrometry* **17**, 2483–2487.
- R-Core-Team (2013) *R: A Language and Environment for Statistical Computing*. Vienna: R Foundation for Statistical Computing.
- Raina J-B, Tapiolas DM, Foret S, Lutz A, Abrego D, Ceh J, Seneca FO, Clode PL, Bourne DG, Willis BL and Motti CA (2013) DMSP biosynthesis by an animal and its role in coral thermal stress response. *Nature* **502**, 677–680.
- Ralph PJ and Gademann R (2005) Rapid light curves: a powerful tool to assess photosynthetic activity. *Aquatic Botany* **82**, 222–237.
- Saroussi S and Beer S (2007) Alpha and quantum yield of aquatic plants derived from PAM fluorometry: uses and misuses. *Aquatic Botany* **86**, 89–92.
- Sathyendranath S and Platt T (1988) The spectral irradiance field at the surface and in the interior of the ocean: a model for applications in oceanography and remote sensing. *Journal of Geophysical Research* **93**, 9270.
- Schreiber U (2004) Pulse-Amplitude-Modulation (PAM) fluorometry and saturation pulse method: an overview. In Papageorgiou GC and Govindjee (eds) *Chlorophyll A Fluorescence*. Dordrecht: Springer, pp. 279–319.
- Sebens KP and Johnson AS (1991) Effects of water movement on prey capture and distribution of reef corals. *Hydrobiologia* **226**, 91–101.
- Sebens KP, Helmuth B, Carrington E and Agius B (2003) Effects of water flow on growth and energetics of the scleractinian coral *Agaricia tenuifolia* in Belize. *Coral Reefs* **22**, 35–47.
- Semmler RF, Hoot WC and Reaka ML (2016) Are mesophotic coral ecosystems distinct communities and can they serve as refugia for shallow reefs? *Coral Reefs* **36**, 1–12.
- Shimamura M, Irino T, Oba T, Xu G, Lu B, Wang L and Toyoda K (2008) Main controlling factors of coral skeletal carbon isotopic composition and skeletal extension rate: high-resolution study at Hainan Island, South China Sea. *Geochemistry Geophysics Geosystems* **9**, 1–11.
- Shlesinger T, Gribblat M, Rapuano H, Amit T and Loya Y (2018) Can mesophotic reefs replenish shallow reefs? Reduced coral reproductive performance casts a doubt. *Ecology* **99**, 421–437.
- Silsbe GM and Malkin SY (2015) phytools: phytoplankton production tools. An R package available on CRAN: <https://cran.r-project.org/web/packages/phytools/index.html>.
- Suarez RK, Darveau C-A and Childress JJ (2004) Metabolic scaling: a many-splendored thing. *Comparative Biochemistry and Physiology Part B: Biochemistry and Molecular Biology* **139**, 531–541.
- Sunda W, Kieber DJ, Kiene RP and Huntsman S (2002) An antioxidant function for DMSR and DMS in marine algae. *Nature* **418**, 317–320.
- Szmant AM and Gassman NJ (1990) The effects of prolonged bleaching on the tissue biomass and reproduction of the reef coral *Montastrea annularis*. *Coral Reefs* **8**, 217–224.

- Torres ME, Mix AC and Rugh WD** (2005) Precise $\delta^{13}\text{C}$ analysis of dissolved inorganic carbon in natural waters using automated headspace sampling and continuous-flow mass spectrometry. *Limnology and Oceanography: Methods* **3**, 349–360.
- Veron JEN, Stafford-Smith MG, Turak E and DeVantier LM** (2016) *Agaricia lamarcki*, Milne Edwards and Haime, 1851. In *Corals of the World*. Available at http://www.coralsoftheworld.org/species_factsheets/species_factsheet_summary/agaricia-lamarcki/?version=0.01.
- Waldron S, Marian Scott E, Vihermaa LE and Newton J** (2014) Quantifying precision and accuracy of measurements of dissolved inorganic carbon stable isotopic composition using continuous-flow isotope-ratio mass spectrometry. *Rapid Communications in Mass Spectrometry: RCM* **28**, 1117–1126.
- Wangpraseurt D, Lichtenberg M, Jacques SL, Larkum AW and Kühl M** (2019) Optical properties of corals distort variable chlorophyll fluorescence measurements. *Plant Physiology* **179**, 1608–1619.
- Werner RA and Brand WA** (2001) Referencing strategies and techniques in stable isotope ratio analysis. *Rapid Communications in Mass Spectrometry* **15**, 501–519.
- Yang T and Jiang S-Y** (2012) A new method to determine carbon isotopic composition of dissolved inorganic carbon in seawater and pore waters by CO_2 – water equilibrium. *Rapid Communications in Mass Spectrometry* **26**, 805–810.